JOURNAL OF MATERIALS SCIENCE 17 (1982) 1329–1336

Direct comparison of the loss of load transfer to "E" and "S" glass fibres manufactured by drawing into different environments

M. D. VAUDIN*, K.H.G. ASHBEE
University of Bristol, H H Wills Physics Laboratory, Tyndall Avenue, Bristol, UK

Accelerated water uptake tests have been used to compare the onsets of destruction of the ability to transfer shear stress at fibre/matrix interfaces in epoxy matrix glass reinforced plastic (GRP) manufactured with each of four different fibres. The ability to transfer shear stress has been monitored directly by measurement of stress birefringence through and adjacent to individual fibres. Full theoretical and practical details of the experimental method are given. "S" glass fibres, drawn into an atmosphere of ammonia in an attempt to promote the deposition of primary amines and/or secondary amines, rapidly lose their ability to receive shear stress from the matrix. This is attributed to neutralization of CO_2 by NH_3 within interfacial pockets of dissolved water, and the associated generation of osmotic pressure. Commercial samples of "S" and "E" glass fibres and "E" glass fibres drawn into an atmosphere of ammonia, all survive much larger water uptakes although, in the case of both kinds of "E" glass fibre, immersion in boiling water eventually gives rise to interfacial pressure pockets. These pressure pockets are also attributed to osmosis, with the role of dissolved solutes tentatively ascribed to the modifying agents present in "E" glass formulations.

1. Introduction

In an experiment designed to encourage the formation of amines and diamines on the surface of glass fibres, Martin [1] drew into an atmosphere of ammonia, fibres from marbles of "E" glass and "S" glass supplied by Owens Corning Fibreglas (OCF). If successful, it was anticipated that the presence of surface amines would promote chemical bonding to composite matrix materials such as epoxy resins. It is the durability of such and any other bonds, if they exist, in epoxy resin composites exposed to hot aqueous environments that is evaluated here.

The photoelastic technique first used by Ashbee and Wyatt [2] to study the deterioration of load transfer during water uptake by "E" glass fibre/polyester resin composites, is fully described and then used to assess the degradation by diffused water of identical epoxy matrix composites prepared with "E" and "S" glass fibres, some commercial grades supplied by OCF and others drawn into an ammonia atmosphere at Iowa State University.

2. Poincaré sphere construction

The state of stress generated in a glass fibre/epoxy resin composite during resin cure and during subsequent cooling to room temperature is complex. Its analysis using polarized light is simplified by means of the Poincaré sphere construction [3]. A single point on the surface of the sphere represents the polarization of electromagnetic oscillation at any point in the system. Any change in this polarization is represented

*Present address: Department of Materials Science, Cornell University, Ithaca, NY 14853, USA.

0022–2461/82/051329–08$03.46/0

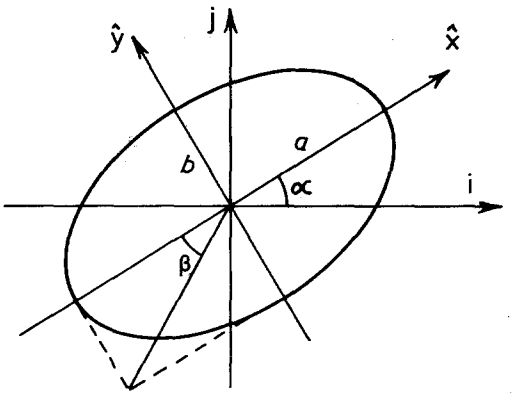

Figure 1 Projection of the E vector helix.

by displacement of the point across the surface of the sphere in accordance with the following simple rules. For a polarized light wave, the end point of the electric vector, **E**, describes an elliptical helix and this helix projects onto a plane parallel to the wavefront as an ellipse whose eccentricity is defined by the angle $\beta = \tan^{-1}(b/a)$, where a and b are the lengths of the semi-major and semi-minor axes. The orientation of the ellipse with respect to some arbitrary Cartesian basis (**i**, **j**) normal to the optic axis, is specified by the angle α (Fig. 1). The point, P, representing the state of polarization defined by the angles α and β is plotted on the surface of a unit sphere at a latitude of 2β relative to the equator and a longitude of 2α relative to some arbitrary meridian (Fig. 2). By convention, points in the upper hemisphere are used to represent electromagnetic radiation in which the **E** vector rotates anti-clockwise, and those in the lower hemisphere are used to represent electromagnetic radiation in which **E** rotates clockwise.

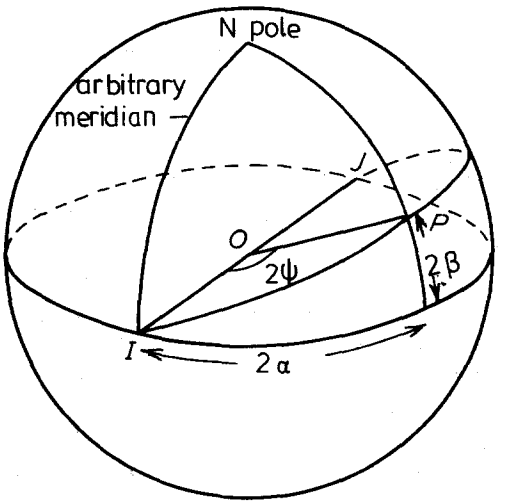

Figure 2 Poincaré sphere construction.

Poincaré's construction has several consequences that are immediately obvious. All points lying on the equator represent linearly polarized light; the two poles (north and south) represent circularly polarized light rotating anti-clockwise and clockwise respectively; points having the same latitude (β = constant) represent ellipses of the same ellipticity but different orientations and points having the same longitude (α = constant) represent ellipses of different ellipticities but with the same orientation; points at the opposite ends of a diameter to the sphere represent elliptical helices of opposite handedness – the ellipses have identical shape but the major axis of one coincides with the minor axis of the other.

This last property of the construction has an important special case when the diameter is a diameter to the equator, since the ends of the diameter then represent two waves linearly polarized at right angles. These waves can combine to generate any elliptically polarized wave and the Poincaré sphere can be used to determine the phase and amplitude relationships between them. Thus, in Fig. 2, I and J represent two linearly polarized waves and P represents the elliptically polarized wave to be generated. Conversely, P represents a polarized wave, ellipticity angle β, which is to be resolved into two orthogonal linearly polarized components in the directions **i** and **j**, α clockwise and $(90-\alpha)$ anti-clockwise from the major axis (Fig. 1). In both cases the construction is the same. The vector **E** of an elliptically polarized electro-magnetic wave as a function of time is

$$\mathbf{E}(t) = a\cos\omega t\,\hat{\mathbf{x}} + b\sin\omega t\,\hat{\mathbf{y}}, \qquad (1)$$

where $\hat{\mathbf{x}}$ and $\hat{\mathbf{y}}$ are unit vectors parallel to the major and minor axes whose lengths are a and b respectively (See Fig. 1). Using axes **i** and **j** inclined at α to $\hat{\mathbf{x}}$ and $\hat{\mathbf{y}}$, **E** can be expressed as

$$\mathbf{E}(t) = A\cos(\omega t - \theta_1)\mathbf{i} + B\cos(\omega t - \theta_2)\mathbf{j}, \qquad (2)$$

where θ_1 and θ_2 are the phase angles and A and B are the amplitudes of the two waves. To compare these two expressions we express $\hat{\mathbf{x}}$ and $\hat{\mathbf{y}}$ as follows

$$\begin{aligned}\hat{\mathbf{x}} &= \cos\alpha\,\mathbf{i} + \sin\alpha\,\mathbf{j}\\ \hat{\mathbf{y}} &= -\sin\alpha\,\mathbf{i} + \cos\alpha\,\mathbf{j}.\end{aligned} \qquad (3)$$

Substituting Equation 3 into Equaton 1

we obtain

$$\mathbf{r} = (a\cos\omega t\cos\alpha - b\sin\omega t\sin\alpha)\mathbf{i} + (a\cos\omega t\sin\alpha + b\sin\omega t\cos\alpha)\mathbf{j}. \quad (4)$$

Expanding Equation 2 and comparing terms with Equation 4 yields

$$\begin{aligned} a\cos\alpha &= A\cos\theta_1, \\ b\sin\alpha &= -A\sin\theta_1, \\ a\sin\alpha &= B\cos\theta_2 \end{aligned} \quad (5)$$

and

$$b\cos\alpha = B\sin\theta_2.$$

By eliminating θ_1 and θ_2 the following equations are obtained

$$\begin{aligned} A^2 + B^2 &= a^2 + b^2 \\ A^2 - B^2 &= (a^2 - b^2)\cos 2\alpha. \end{aligned} \quad (6)$$

and

Putting $B/A = \tan\psi$ these two equations can be reduced to

$$\cos 2\psi = \cos 2\beta\cos 2\alpha.$$

In the spherical triangle IPQ (Fig. 3)

$$\cos I\hat{O}P = \cos 2\beta\cos 2\alpha,$$

hence $2\psi = I\hat{O}P$ which determines the relative amplitudes of the two waves. From Equations 5 and 6 it can be shown that

$$\frac{2ab}{a^2+b^2} = \frac{2AB}{A^2+B^2}\sin(\theta_2 - \theta_1)$$

and

$$(a^2 - b^2)\tan\alpha = \frac{2AB}{A^2 - B^2}\cos(\theta_2 - \theta_1),$$

which, on rearranging, become

$$\sin 2\beta = \sin 2\psi\sin(\theta_2 - \theta_1)$$

and

$$\tan 2\alpha = \tan 2\psi\cos(\theta_2 - \theta_1).$$

In the spherical triangle IPQ

$$\sin 2\beta = \sin 2\psi\sin\theta$$

and

$$\tan 2\alpha = \tan 2\psi\cos\theta,$$

where θ is the angle between the equatorial plane and the plane containing I, J and P.
Hence, $\theta = \theta_2 - \theta_1$, indicating that the wave represented by J lags by θ behind the wave I.

On entering a bi-refringment material, polarized light can be considered as resolved into two components, parallel to the fast and slow axes of the material in the plane normal to the optic axis. The phase and amplitude relationships between the two waves are given by the angles θ and ψ described above. The two waves pass through the crystal at different velocities, their relative amplitudes remain the same but the phase difference between them changes by an angle, $\delta\theta$, proportional to the thickness, e, of material traversed and to the difference in magnitude of the refractive index in the fast and slow directions, Δn. In the Poincaré sphere representation, ψ remains constant and θ changes by $\delta\theta = 2\pi\Delta ne/\lambda$ radians. Assuming I and J to be the fast and slow directions respectively (Fig. 3), the position of P, which represents the incident light, is rotated by $\delta\theta$ anti-clockwise about the axis IJ as indicated.

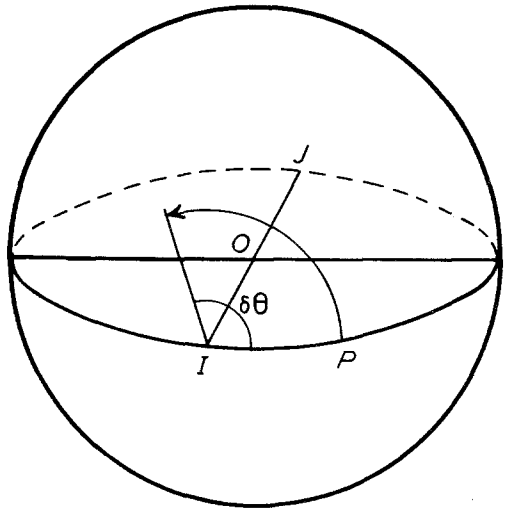

Figure 3 Effect of retardation on elliptically polarized light.

3. The origin of birefringence in short fibre composites

Stress-free glass and stress-free glassy resins are optically isotropic materials. However, during manufacture of a composite material, and especially during cooling from the resin cure temperature, there occurs a net shrinkage of resin onto the fibres, the consequence of which is that both materials are rendered optically anisotropic, i.e. birefringent.

Of special interest, since it affords a direct method for the detection and monitoring of load transfer from matrix to fibre, is the birefringence measured through adjacent diameters

in individual short fibres. The magnitude of this birefringence is a measure of the local axial stress in the fibre [2] which, since it arises mainly by way of shear stress transmitted across the cylindrical part of the fibre/matrix interface, builds-up from the fibre ends towards the fibre centre. Any deterioration in the efficiency of interfacial load transfer reduces the build-up of optical retardation measured through adjacent diameters. In practice, a convenient load transfer index (LTI) is simply the difference between the optical retardation measured through a diameter at the fibre centre and that measured through a diameter close to either fibre end, both measurements being corrected for resin birefringence by subtracting the optical retardation measured through resin immediately adjacent to the fibre diameter concerned.

In principle, each retardation can be evaluated by calculating an integral along the light path and each corresponds to a curve on the Poincaré sphere. The retardation of light passing through the fibre has components due to the differences between (a) the hoop and axial stresses (both tensile) in the resin, and (b) the hoop and axial stresses (both compressive) in the fibre. Retardation in resin next to the fibre centre is relatively simple to measure since the axial tension and the resultant of hoop and radial stresses are always aligned with the crossed polars. In resin near the fibre ends, the situation is complicated by the presence of shear stresses and strains which result in the principle stress directions not being aligned parallel to the fibre.

The magnitudes of these various stresses are initially determined by a combination of the fibre geometry, the difference in thermal expansion coefficients between resin and glass, and the location of the fibre within the resin slab (during casting, fibres tend to settle between 5 and 20 micrometres from the bottom of the specimen). By symmetry, the interfacial shear stress at the centre of the fibre is zero. Mismatch between fibre and resin as a result of resin shrinkage increases with distance, x, from the fibre centre-producing shear stresses which, according to Cox [4], are proportional to $\sinh(x)$. The radial compressive and hoop tensile stresses in the resin are, according to simple theories, equal in magnitude and both fall off as $1/r$ where r is the radial distance from the fibre axis. Their magnitudes are expected to depend on fibre thickness, being greatest for the 13 μm laboratory "S" glass fibres and least for the 6 μm laboratory "E" glass fibres. This was borne out by experimental observation in that the retardation in the resin next to the fibre centre differed from the background retardation by 11.5 nm for the laboratory "S" glass fibre, by 5.85 nm for the commercial "S" glass fibre and 1.5 nm for laboratory "E" glass fibre. The variation of retardation with radial distance from the axis of the laboratory "S" glass fibre is shown in Fig. 4 and shows the expected $1/r$ dependence.

4. Experimental procedure

The fibres studied were of four types: commercial "E" and "S" glass, and "E" and "S" glass drawn in a dry ammonia atmosphere. The two laboratory fibres, supplied by Professor David Martin, Iowa State University, Ames, Iowa, were 6 μm diameter for the "E" glass and 13 μm diameter for the "S" glass. The commercial fibres were nominally 10 μm in diameter. Small quantities of all four fibres were cut into 1 to 2 mm lengths, washed in acetone, dried in an oven and introduced into the epoxy resin mix prior to vigorous stirring and subsequent de-gassing under vacuum. Specimens were cast in silicon rubber moulds which had been cleaned and dried, and warmed to approximately 50° C to aid flow of the viscous resin. After gelling for 2 h at 100° C, the oven temperature was slowly raised to 150° C and the specimens cured for a further 4 h. Each measurement of LTI entailed a minimum of nine compensation readings, three at each end and three in the middle of the fibre. A corrected retardation was also obtained approximately mid-way between the middle and one end.

5. Evaluation of the technique

The magnitude of the birefringence in an around totally embedded fibres is small, being in the grey region of the Michel–Lèvy chart, and is conveniently measured with a Brace–Köhler compensator. This consists of a slice of birefringent crystal which introduces a known retardation, R_o, between light waves polarized in the fast and slow directions of the crystal. It is usually calibrated for a single wavelength of light and the retardation is normally quoted in nanometres of path difference. Initially the compensator is aligned with its fast and slow axes parallel to the axes of the crossed polars and the fast axis of the specimen is set at 45° to the polars. The compensator is then rotated through an angle

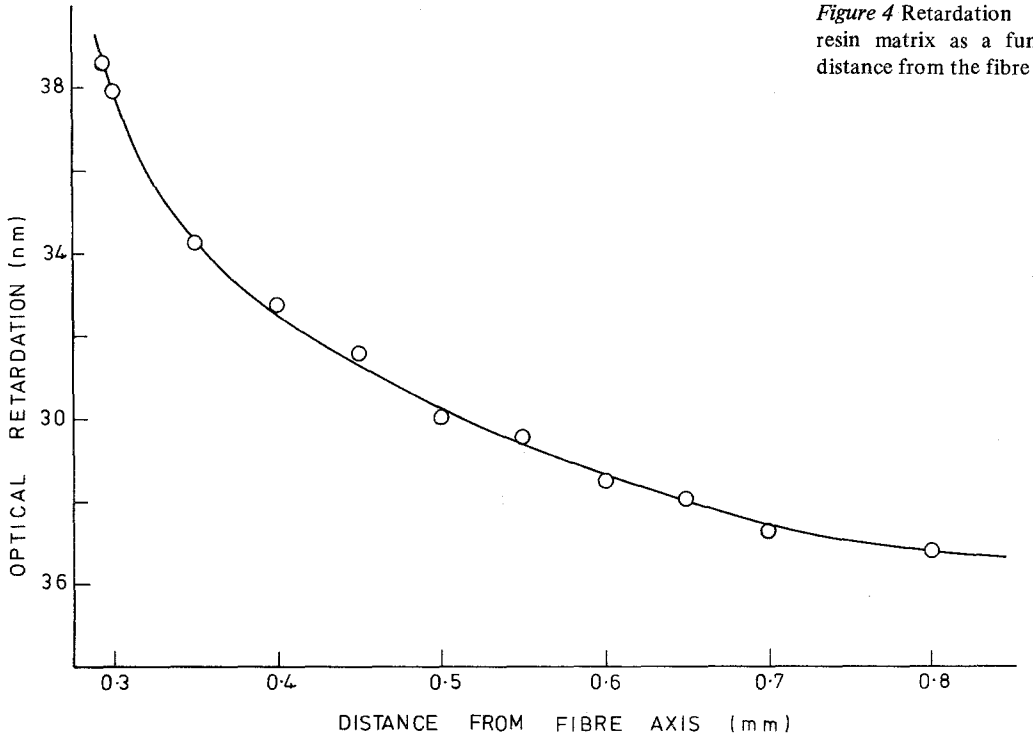

Figure 4 Retardation in the resin matrix as a function of distance from the fibre axis.

ψ until the intensity of light passing through the whole system is a minimum; the retardation due to the specimen is $R \sim R_o \sin 2\psi$. The Poincaré sphere analysis of the experimental system is shown in Fig. 5. P and A represent the directions of the polarizer and analyser respectively. The point P denoting light emerging from the polarizer is displaced by rotating the compensator through an angle θ equal to $2\pi R_o/\lambda$ about an axis CC' lying in the equatorial plane at an angle 2ψ to the line PA; hence P moves to P'. The specimen rotates the point P' through an angle β equal to $2\pi R/\lambda$ about the axis SS' (perpendicular to AP) to a point P'' such that $P\hat{O}P''$ is a minimum, the condition for minimum light intensity transmitted through the analyser. Hence P'' must lie on the equatorial circle. It is easily shown that

$$\cot\theta \sin\beta = \cos\theta \sin 2\psi,$$

from which we obtain

$$\sin\beta = \sin\theta \sin 2\psi.$$

For small retardations,

$$R \sim R_o \sin 2\psi.$$

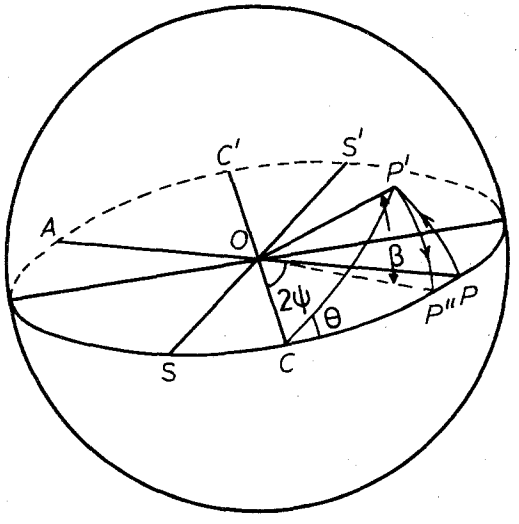

Figure 5 Poincaré sphere analysis of retardations through and adjacent to individual fibres.

Fig. 6 shows the pattern of stress-induced birefringence in and around one of the short "S" glass fibres manufactured by drawing into an ammonia atmosphere, and totally embedded in a slab of Ciba Geigy MY 750 epoxy resin; the fibre axis is aligned parallel to one of the crossed polars. All compensation measurements were taken with the fibre at 45° to the crossed polar axes, except where stated otherwise.

Even with slow cooling in the oven, the specimens possessed intrinsic birefringence with the

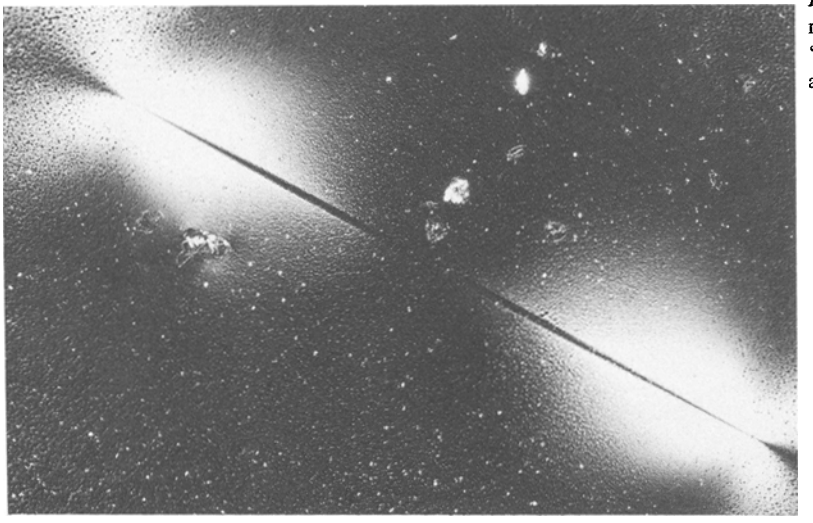

Figure 6 Stress induced birefringence in and around an "S" glass fibre drawn into an atmosphere of ammonia.

fast axis approximately parallel to the largest of the mould dimensions. This is attributed to the difference in contraction between resin and mould. The magnitude of the background birefringence was at least double the largest measurable stress-induced local birefringence arising from resin shrinkage onto a fibre. For this reason, the pattern of isoclinics in and around any individual fibre was cylindrically symmetric only when the fibre was approximately parallel to the fast or slow axes of the background birefringence. With this special geometry the fast axes in the resin either side of the fibre end were misoriented from the fibre axis by equal but opposite angles ($\pm \delta$), and from the Poincaré sphere construction it can be shown that the compensations measured in these particular regions of resin should be multiplied by $\sec(2\delta)$ to find the true stress-induced birefringences. This theoretical prediction was confirmed experimentally by measurements taken from a commercial "E" glass fibre oriented at 6° to the specimen axis. 6° is sufficiently near parallel to produce a cylindrically symmetrical pattern of isoclinics, as in Fig. 6. As stated above, the normal orientation for taking compensation readings was at 45° to this position of symmetry. However, rotating the specimen 19.3° clockwise from the "normal" position oriented the fast axis of the resin on one side of a fibre end at 45° to the crossed polars and changed the measured birefringence from 19.5 nm to 25 nm. Similarly, a rotation anticlockwise of 21.2° correctly oriented the resin on the other side of the fibre and changed the retardation from 17.0 nm to 23.25 nm. From the ratios of uncorrected to corrected retardations, the Poincaré sphere construction predicts misorientation angles of 19.37° and 21.51°, i.e. close to the recorded angles.

6. Results

Fig. 7 summarizes the data obtained during 170 hours of immersion in water at 60° C. The large variations in load transfer index which occured in all cases during the first 1500 min is not wholly attributable to experimental error which was ± 2 nm for the LTI. The general downward trend of each graph is overlaid with fluctuations associated with changes in stress optic coefficient and with resin swelling. The thinner "E" glass laboratory drawn fibres appear to have the smallest load transferred to them, and the "S" glass laboratory drawn fibres initially had higher values of LTI than the "S" glass commercial fibres. However, during water immersion, interfacial bubbles developed on the two "S"-in-ammonia fibres, indicating the onset of debonding particularly near the fibre ends. Fig. 8 is an optical micrograph of one of these fibres after 6400 min immersion. The load transfer index reflected this deterioration, falling to 3.4 nm for the fibre in Fig. 8 and to 1.1 nm for the other fibre. The remaining fibres all experienced an initial slight drop in LTI but during the final 80 % of the immersion time there was no significant change.

The specimens were subsequently placed in boiling water for 1 min and then left in the water as it slowly cooled. The effect of this treatment

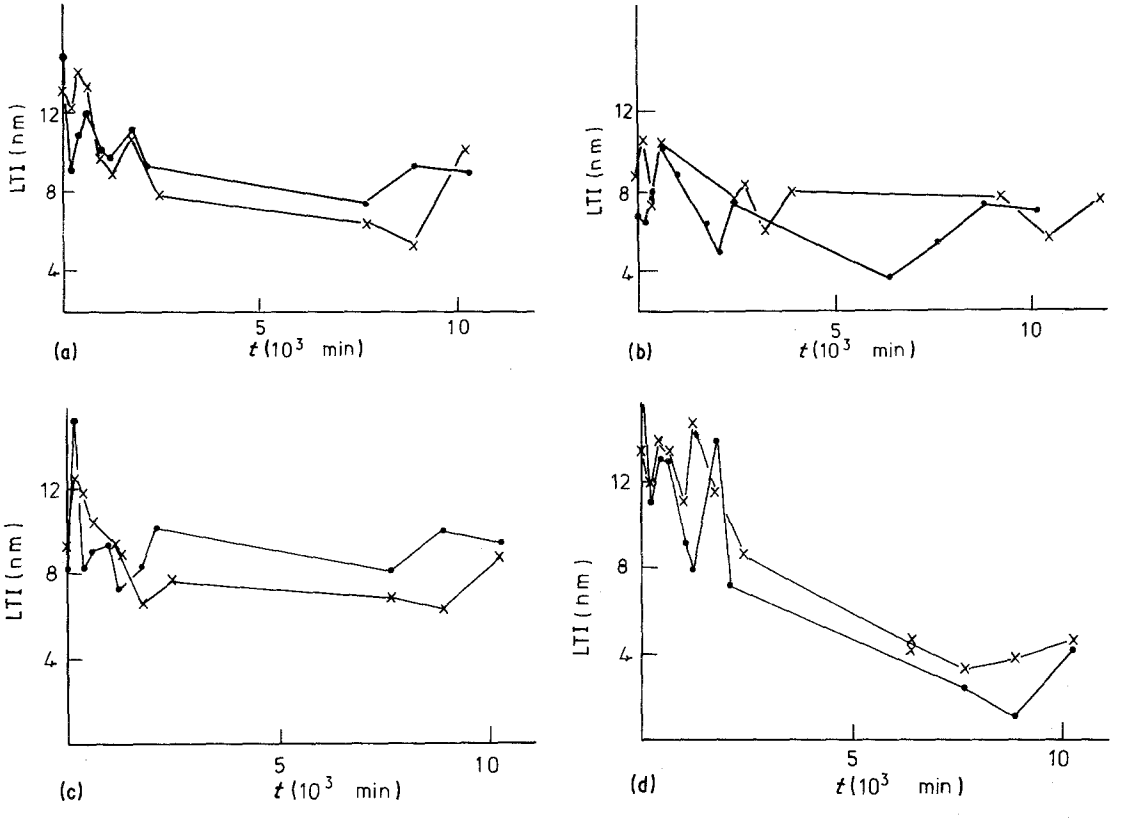

Figure 7 Load transfer index (LTI) against time of immersion (t) of MY750 matrix composites in water of 60° C. (a) Commercial "E" glass fibre, (b) "E" glass fibre drawn into ammonia, (c) commercial "S" glass fibre, (d) "S" glass fibre drawn into ammonia.

was in some cases considerable, as can be seen from the micrograph in Fig. 9, which is an "E" glass fibre drawn in ammonia. The commercial "S" glass fibres were hardly affected by the boiling treatment.

The fibre in Fig. 10 was photographed between crossed-polars and is surrounded by a symmetrical pattern of isoclinics similar to Fig. 6 but the fibre itself is not completely dark. Rotating the specimen 4° clockwise rendered the fibre dark but destroyed the cylindrical symmetry of the resin pattern. This is an example of slight misalignment between the stress-induced and background bi-

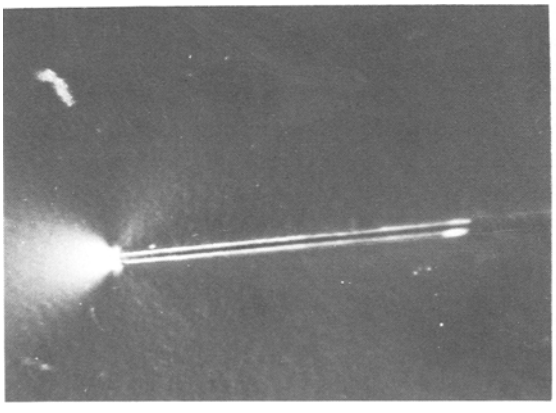

Figure 8 "S" glass fibre drawn into ammonia, after 6400 min immersion of the composite in water at 60° C.

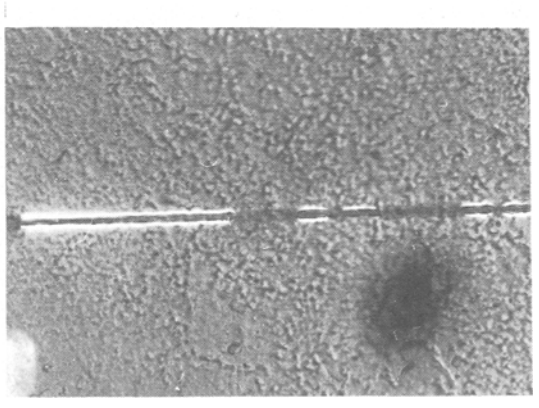

Figure 9 "E" glass fibre drawn in ammonia, after 10200 min immersion in water at 60° C.

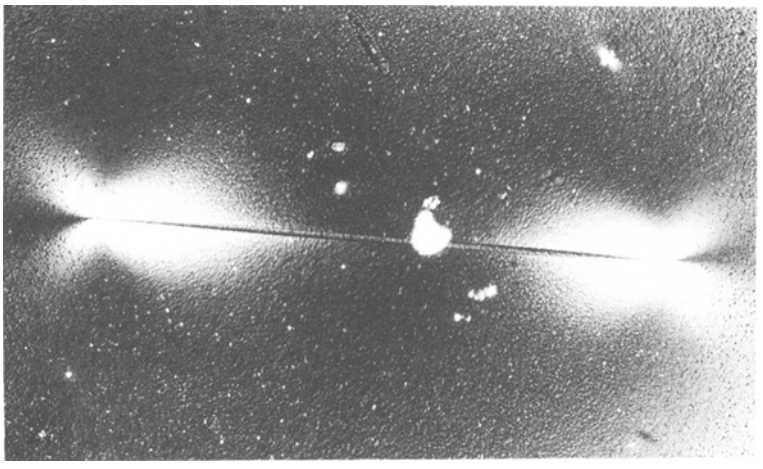

Figure 10 Isoclinics in and around a fibre misaligned with the background birefringence of matrix resin.

refringence. In more extreme cases, it was not possible to orient the fibre so that the isoclinics ever display cylindrically symmetry. The isoclinics are always zero-order but because of the background birefringence they do not necessarily indicate regions of the specimen in which the principle stress directions are aligned with the crossed polars.

7. Discussion

The early appearance of interfacial pressure pockets in composites manufactured from "S" glass fibres drawn into ammonia is interesting. One mechanism which would account for this observation is osmosis caused by the reaction

$$NH_3 + CO_2 + H_2O \rightarrow NH_4^+ + HCO_3^-.$$

MgO is a major constituent of "S" glass and, in accordance with normal glass-making practice, is probably introduced as $MgCO_3$. If true, some of the CO_2 liberated by thermal decomposition during glass melting will be retained as dissolved gas. Ammonia is expected to be present as gas adsorbed by the glass during fibre drawing. Subsequent dissolution of solutes at the resin/fibre interface will lower the chemical potential of the water. To counteract this, and thereby maintain chemical equilibrium, the pressure of the pockets of interfacial solution rises above that of the outside water.

The absence of ammonia in OCF "S" glass fibre precludes the possibility of formation of ammoniacal solutions by water which has diffused to fibre surfaces. In the case of "E" glass fibres drawn into ammonia, the non-occurrence of interfacial pockets of ammoniacal solution is attributed to the absence of CO_2. However, in the case of "E" glass fibre composites, dissolved water at its boiling point eventually finds sufficient water soluble constituents (presumably $Na_2O + K_2O$ extracted from the glass) to form interfacial pressure pockets.

Acknowledgements

One of us (MDV) was supported by US Army grant number DA-ERO-78-G-117 monitored by Dr N. Schneider of the Army Materials and Mechanics Research Center. The authors also gratefully acknowledge the receipts of samples of fibres from Professor D. Martin, Iowa State University.

References

1. D. MARTIN, Proceedings of the 3rd Annual US Army Composite Materials Research Review October 1980, Williamstown, Massachusetts.
2. K. H. G. ASHBEE and R. C. WYATT, *Proc. Roy. Soc.* **A312** (1969) 553.
3. H. POINCARÉ, "Théorie Mathématique de la Lumiére" (Gauttie-Villars, Paris, 1892).
4. H. L. COX, *Brit. J. Appl. Phys.* **3** (1952) 72.

Received 1 September
and accepted 28 September 1981